ANALYTICAL TECHNIQUES TO EVALUATE THE INTEGRALS OF 3D AND 2D SPATIAL DYADIC GREEN'S FUNCTIONS

G. Gao and C. Torres-Verdín

Department of Petroleum and Geosystems Engineering
1 University Station, Mail Stop C0300
The University of Texas at Austin
Austin, TX 78712, USA

T. M. Habashy

Schlumberger-Doll Research
Old Quarry Road, Ridgefield, CT 06877, USA

Abstract—The Dyadic Green's function is in general viewed as a generalized, or distribution function. A commonly used procedure to evaluate its volume integral is the principal-volume method, in which an infinitesimal volume around the singularity is excluded from the integration volume. In this paper, we develop a general analytical technique to evaluate the integral of the dyadic Green's function without the need to specify an exclusion volume.

The newly derived expressions accurately integrate the singularity and can be used for integration over any shape of spatial discretization cell. We derive explicit expressions for the integral of the 3D dyadic Green's function over a sphere and over a general rectangular block. Similar expressions are obtained for the 2D dyadic Green's function over a cylinder and over a general rectangular cell. It is shown that using the integration technique described in this paper for spherical/circular cells, simple analytical expressions can be derived, and these expressions are exactly the same as those obtained using the principal-volume method. Furthermore, the analytical expressions for the integral of the dyadic Green's function are valid regardless of the location of the observation point, both inside and outside the integration domain. Because the expressions only involve surface integrals/line integrals, their evaluation can be performed very efficiently with a high degree of accuracy. We compare our expressions against the equivalent volume approximation for a wide

range of frequencies and cell sizes. These comparisons clearly show the efficiency and accuracy of our technique.

It is also shown that the cubic cell (3D) and the square cell (2D) can be approximated with an equivalent spherical cell and circular cell, respectively, over a wide range of frequencies. The approximation can be performed analytically, and the results can be written as the value of the dyadic Green's function at the center multiplying a "geometric factor". We describe analytical procedures to derive the corresponding geometric factors.

Appendix E. Derivation of the Explicit Expressions of the Integral of the Dyadic Green's Function over a General Rectangular Block Using the General Formula

Appendix F. Derivation of the Explicit Expressions for the Integral of the Dyadic Green's Function over a General Rectangular Cell (Rectangular Cylinder)

References

1. INTRODUCTION

Integral equations have been widely used to solve electromagnetic (EM) scattering and related problems, such as those arising in antenna design, geophysical subsurface sensing [9–11], biomedical engineering [8], and optical scattering [14], to name a few. A fundamental component of the integral equation is the dyadic Green's function, which makes it possible for the integral equation to exhibit a simple analytical form. This feature is especially true for multiple scattering problems, in which the complex physics of a vector field is properly synthesized by the dyadic Green's function [1].

The study of dyadic Green's functions has attracted numerous researchers in the EM community [1–8]. Dyadic Green's functions can be classified into a spatial representation, in which the function is written in terms of simple algebraic expressions in the coordinate space r, and an eigenfunction representation, in which the function is written in terms of vector wave functions or eigenfunctions suitable for the assumed geometry [1]. Chew [1] gives a review of these two representations of the dyadic Green's function and of their relationships.

This paper is devoted to the spatial representation of the dyadic Green's function in an unbounded homogeneous and isotropic conductive medium. In this case, the dyadic Green's function can be derived in closed form using vector and scalar potential theory [2]. A fundamental feature of the dyadic Green's function is the singularity in the source region. This feature has been extensively studied by Yaghjian [3, 4] and Van Bladel [2], among others. Their work has shown that the dyadic Green's function can only be viewed as a generalized function involving a Dirac delta function singularity and is only valid in the distribution sense. Its evaluation should be approached using a method called "Principal Volume Method," in which an exclusion volume is specified around the singularity. As for the principal volume integration, an equivalent volume (sphere in 3D and circle in 2D) approximation has been frequently used for

some special shapes of discretization cell given that, for those cases, analytical solutions can be derived to simplify the evaluation [5, 6, 8]. This paper reviews the derivation of the expressions for the equivalent volume approximation in the source region and outside the source region using various methods, both for 3D and 2D cases. We remark that the singularity property of the dyadic Green's function has led to the formulation of the Extended Born Approximation in EM scattering [15, 16].

The principal volume method, so far, is about the only method available to solve the integral of the dyadic Green's function in the source region. In this paper, we show that the principal volume is actually not necessary. Our derivation is valid for the integration over any shape of discretization cell and for any spatial location, both for 3D and 2D domains. We give explicit expressions for the integration over a spherical cell (circular cell in 2D) and a general rectangular cell (square cell in 2D). It is shown that the expression for a sphere/circle from our formula gives exactly the same solution as the principal volume method for the same cell. Our formula is also validated numerically by comparing the numerical results to those obtained from an already-validated code and the principal volume method for a wide range of frequencies and cell sizes, both in the source region and outside the source region. For a cubic/square cell, when the observation points are outside the source region, we derive a geometric factor solution, which is nothing but the dyadic Green's function in the geometric center of the cell multiplying a geometrical factor. The formulas reported here have been used to simulate tri-axial induction tool measurements acquired in inhomogeneous and electrically anisotropic rock formations [9–11].

2. THE DYADIC GREEN'S FUNCTION

Assume an EM source that exhibits a time harmonic dependence of the type $e^{-i\omega t}$, where ω is angular frequency, t is time, and $i = \sqrt{-1}$. The magnetic permeability of the medium equals that of free space, μ_0. Thus, the integral equation for electric and magnetic fields can be written in general as [2, 3, 12]

$$\boldsymbol{E}(\boldsymbol{r}) = \boldsymbol{E}_b(\boldsymbol{r}) + \int_\tau \overline{\overline{G}}^e(\boldsymbol{r}, \boldsymbol{r}_0) \cdot \Delta\overline{\overline{\sigma}}(\boldsymbol{r}_0) \cdot \boldsymbol{E}(\boldsymbol{r}_0)d\boldsymbol{r}_0, \qquad (1)$$

and

$$\boldsymbol{H}(\boldsymbol{r}) = \boldsymbol{H}_b(\boldsymbol{r}) + \int_\tau \overline{\overline{G}}^h(\boldsymbol{r}, \boldsymbol{r}_0) \cdot \Delta\overline{\overline{\sigma}}(\boldsymbol{r}_0) \cdot \boldsymbol{E}(\boldsymbol{r}_0)d\boldsymbol{r}_0, \qquad (2)$$

where $\boldsymbol{E}(\boldsymbol{r})$ and $\boldsymbol{H}(\boldsymbol{r})$ are the electric and magnetic field vectors, respectively, at the measurement location, $\boldsymbol{r}$. In the above equations, $\boldsymbol{E}_b(\boldsymbol{r})$ and $\boldsymbol{H}_b(\boldsymbol{r})$ are the electric and magnetic field vectors, respectively, associated with a homogeneous, unbounded, and isotropic background medium of dielectric constant ε_{rb} and Ohmic conductivity σ_b'. Accordingly, the background complex conductivity is given by $\sigma_b = \sigma_b' - i\omega\varepsilon_{rb}\varepsilon_0$, and the wavenumber k_b, of the background medium is given by $k_b^2 = i\omega\mu_0\sigma_b = \omega^2\mu_0\varepsilon_0\varepsilon_{rb} + i\omega\mu_0\sigma_b'$.

The electric dyadic Green's function included in equation (1) can be expressed in a closed form as

$$\overline{\overline{G}}^e(\boldsymbol{r}, \boldsymbol{r}_0) = i\omega\mu_0 \left(\overline{\overline{I}} + \frac{1}{k_b^2}\nabla\nabla \right) g(\boldsymbol{r}, \boldsymbol{r}_0), \tag{3}$$

where the scalar Green's function $g(\boldsymbol{r}, \boldsymbol{r}_0)$ satisfies the wave equation

$$\nabla^2 g(\boldsymbol{r}, \boldsymbol{r}_0) + k_b^2 g(\boldsymbol{r}, \boldsymbol{r}_0) = -\delta(\boldsymbol{r} - \boldsymbol{r}_0), \tag{4}$$

and whose solution can be explicitly written as

$$g(\boldsymbol{r}, \boldsymbol{r}_0) = \frac{e^{ik_b|\boldsymbol{r}-\boldsymbol{r}_0|}}{4\pi|\boldsymbol{r} - \boldsymbol{r}_0|}. \tag{5}$$

The electric dyadic Green's function is a solution of

$$\nabla \times \nabla \times \overline{\overline{G}}^e(\boldsymbol{r}, \boldsymbol{r}_0) - k_b^2 \overline{\overline{G}}^e(\boldsymbol{r}, \boldsymbol{r}_0) = i\omega\mu_0\delta(\boldsymbol{r} - \boldsymbol{r}_0)\overline{\overline{I}}. \tag{6}$$

The magnetic dyadic Green's function is related to the electric Green's tensor through the expression

$$\overline{\overline{G}}^h(\boldsymbol{r}, \boldsymbol{r}_0) = \frac{1}{i\omega\mu_0}\nabla \times \overline{\overline{G}}^e(\boldsymbol{r}, \boldsymbol{r}_0). \tag{7}$$

Finally, the tensor

$$\Delta\overline{\overline{\sigma}} = \overline{\overline{\sigma}} - \sigma_b\overline{\overline{I}} = \Delta\overline{\overline{\sigma}}' - i\omega\mu_0\Delta\varepsilon_r\varepsilon_0\overline{\overline{I}}. \tag{8}$$

is the complex conductivity contrast within scatterers, with $\Delta\varepsilon_r = \varepsilon_r - \varepsilon_{rb}$, $\Delta\overline{\overline{\sigma}}' = \overline{\overline{\sigma}}' - \sigma_b'\overline{\overline{I}}$, and where $\overline{\overline{I}}$ is a unity dyad.

In the 2D case, the electric dyadic Green's function can be expressed as

$$\overline{\overline{G}}^e(\boldsymbol{\rho}, \boldsymbol{\rho}_0) = i\omega\mu \left(\overline{\overline{I}} + \frac{1}{k_b^2}\nabla\nabla \right) g(\boldsymbol{\rho}, \boldsymbol{\rho}_0), \tag{9}$$

where

$$g(\boldsymbol{\rho}, \boldsymbol{\rho}_0) = \frac{i}{4} H_0^{(1)}(k_b|\boldsymbol{\rho} - \boldsymbol{\rho}_0|) \tag{10}$$

is the 2D scalar Green's function and $H_0^{(1)}(\cdot)$ is the Hankel function of the first kind and order zero, and $\boldsymbol{\rho}$ is the location vector in 2D Cartesian coordinates.

This paper is devoted to equations (3) and (9) only. The description is focused mainly on the 3D dyadic Green's function, because the 2D dyadic Green's function follows the same principles.

3. THE PRINCIPAL VOLUME METHOD

When the source point $\boldsymbol{r}_0$ and the observation point $\boldsymbol{r}$ coincide, equation (1) gives an improper integral, because the double derivatives from $\nabla\nabla$ operating on $g(\boldsymbol{r}, \boldsymbol{r}_0)$ in equation (3) give rise to a singularity of the type $O(1/|\boldsymbol{r} - \boldsymbol{r}_0|^3)$ when $\boldsymbol{r} \to \boldsymbol{r}_0$.

Work by numerous researchers has proved that, although the improper integral in equation (1) does not converge in the classical sense when $\boldsymbol{r} \to \boldsymbol{r}_0$, its principal value integral does exist. The following form of the integral has been suggested [1–4]:

$$\boldsymbol{E}(\boldsymbol{r}) = \boldsymbol{E}_b(\boldsymbol{r}) + PV \int_\tau \overline{\overline{G}}^e(\boldsymbol{r}, \boldsymbol{r}_0) \cdot \Delta\overline{\overline{\sigma}}(\boldsymbol{r}_0) \cdot \boldsymbol{E}(\boldsymbol{r}_0) d\boldsymbol{r}_0 - \frac{\overline{\overline{L}} \cdot \Delta\overline{\overline{\sigma}}(\boldsymbol{r}) \cdot \boldsymbol{E}(\boldsymbol{r})}{\sigma_b}, \tag{11}$$

where $PV \int_\tau [\cdot] d\boldsymbol{r}_0 = \lim_{\tau_\delta \to \infty} \int_{\tau - \tau_\delta} [\cdot] d\boldsymbol{r}_0$ stands for the principal volume integral, and τ_δ is a small exclusion volume. Because the exclusion volume will cause discontinuous currents on the surface of the volume, surface charges will accumulate on the surface, which will cause an electrostatic field inside the volume. This EM field will persist no matter how small the volume is, and is a function of the shape of the volume [1]. The third term in equation (11) gives the correction due to the accumulated surface charges, in which $\overline{\overline{L}}$ is a tensor and is a function of the volume shape.

When using the method of moments [7] to solve equation (11), one frequently faces the problem of evaluating the following improper integral in the 3D case:

$$\overline{\overline{G}}(\boldsymbol{r}) = \int_\tau \overline{\overline{G}}^e(\boldsymbol{r}, \boldsymbol{r}_0) d\boldsymbol{r}_0, \tag{12}$$

and in the 2D case:

$$\overline{\overline{G}}(\boldsymbol{\rho}) = \int_\tau \overline{\overline{G}}^e(\boldsymbol{\rho}, \boldsymbol{\rho}_0) d\boldsymbol{\rho}_0. \tag{13}$$

When $\boldsymbol{r} \to \boldsymbol{r}_0$, using the principal volume method, equation (12) can be evaluated as

$$\overline{\overline{G}}(\boldsymbol{r}) = PV \int_\tau \overline{\overline{G}}^e(\boldsymbol{r}, \boldsymbol{r}_0) d\boldsymbol{r}_0 - \frac{\overline{\overline{L}}}{\sigma_b}. \tag{14}$$

Similarly for the 2D case, when $\boldsymbol{\rho} \to \boldsymbol{\rho}_0$, equation (13) can be evaluated as

$$\overline{\overline{G}}(\boldsymbol{\rho}) = PV \int_S \overline{\overline{G}}^e(\boldsymbol{\rho}, \boldsymbol{\rho}_0) d\boldsymbol{\rho}_0 - \frac{\overline{\overline{L}}_2}{\sigma_b}, \tag{15}$$

where $\overline{\overline{L}}_2$ is a tensor and a function of the exclusion element shape.

When $\boldsymbol{r}/\boldsymbol{\rho}$ is outside the source region, no singularity exists, and the integral in equations (12) and (13) can be evaluated using any numerical method, or analytically for some special cases.

3.1. Equivalent Volume Solution for a Singular Cell

To evaluate the principal value integral in equation (14), numerical methods need to be used in general. However, if we take the exclusion volume as a small sphere (small circle for the 2D case), and approximate the cell using a spherical cell (circular cell for the 2D case) with the equivalent volume (area for the 2D case), an analytical solution can be obtained which has been shown to be a very good approximation for the cubic cell [6, 8] (square cell for the 2D case).

In the 3D case, let $x_1 = x$, $x_2 = y$, $x_3 = z$, $p = 1, 2, 3$, and $q = 1, 2, 3$. The solution of equation (14) can be written as

$$G_{pq} = \frac{\delta_{pq}}{3\sigma_b} \left[2(1 - ik_b a)e^{ik_b a} - 3 \right], \tag{16}$$

where a is the radius of the equivalent sphere, given by

$$a = \left(\frac{3}{4\pi} \right)^{1/3} a_l, \tag{17}$$

and a_l is the side length of the cubic cell. A simplified derivation procedure is given in Appendix A. A more detailed derivation can be found in [5, 6, 8]. Also, an alternative derivation procedure that does not require the specification of the exclusion volume is given in the first part of Appendix B.

In the 2D case, assume an infinite square cylinder parallel to the z direction. The solution of equation (15) can be written as

$$\overline{\overline{G}}(\boldsymbol{\rho}) = \frac{1}{\sigma_b} \left[-1 + \frac{i\pi k_b a H_1^{(1)}(k_b a)}{4} \right] \overline{\overline{I}} + \frac{1}{\sigma_b} \frac{i\pi k_b a H_1^{(1)}(k_b a)}{4} \hat{z}\hat{z}, \tag{18}$$

where $H_1^{(1)}(\cdot)$ is the Hankel function of the first kind and order 1.

A derivation of equation (18) is given in the first part of Appendix C.

3.2. Geometric Factor Solution for Non-Singular Cells

When r/ρ is not in the source region, expressions for the equivalent volume/area approximation can also be derived analytically. As shown in Appendices B and C, the solution of equations (12) and (13) can be written as

$$\overline{\overline{G}}(\boldsymbol{r}) = C^3 \overline{\overline{G}}^e(\boldsymbol{r}, \boldsymbol{r}_c), \tag{19}$$

and

$$\overline{\overline{G}}(\boldsymbol{\rho}) = C^2 \overline{\overline{G}}^e(\boldsymbol{\rho}, \boldsymbol{\rho}_c), \tag{20}$$

where

$\boldsymbol{r}_c$ is the coordinate of the geometric center of the spherical/cubic cell,

$\boldsymbol{\rho}_c$ is the coordinate of the geometric center of the circular/square cell,

and C^3 is the 3D "Geometric Factor" for the integral of the 3D dyadic Green's function, given by

$$C^3 = \frac{4\pi a}{k_b^2} \left[\frac{\sin(k_b a)}{k_b a} - \cos(k_b a) \right], \tag{21}$$

where a is the radius of the cell for a sphere and is given by equation (17) for a cubic cell.

In equation (20), C^2 is the 2D "Geometrical Factor" for the integral of 2D dyadic Green's function, given by

$$C^2 = \frac{2\pi a'}{k_b} J_1(k_b a'), \tag{22}$$

where a' is the radius of the cell for a circular cell and is given by the following formula for a square cell:

$$a' = \frac{a'_l}{\sqrt{\pi}}, \tag{23}$$

where a'_l is the side length of the square. Appendix B gives a detailed derivation of equation (19) and Appendix C gives a detailed derivation of equation (20).

Equations (19) and (20) are referred to as the "Geometric Factor Solutions" in this paper.

4. A GENERAL INTEGRAL EVALUATION TECHNIQUE

The principal volume method uses an exclusion volume to deal with the singularity caused by the dyadic Green's function in the source region. However, it can be shown that the exclusion volume is not needed and that the integral in equations (12) and (13) can be evaluated directly. This is shown next.

First, substitution of equation (3) into equation (12) gives

$$\overline{\overline{G}}(\boldsymbol{r}) = i\omega\mu_0 \left(\overline{\overline{I}} + \frac{1}{k_b^2}\nabla\nabla\right) f(\boldsymbol{r}), \tag{24}$$

where

$$f(\boldsymbol{r}) = \int_\tau g(\boldsymbol{r}, \boldsymbol{r}_0)d\boldsymbol{r}_0. \tag{25}$$

From equation (4), one can obtain

$$g(\boldsymbol{r}, \boldsymbol{r}_0) = -\frac{1}{k_b^2}\delta(\boldsymbol{r} - \boldsymbol{r}_0) - \frac{1}{k_b^2}\nabla^2 g(\boldsymbol{r}, \boldsymbol{r}_0). \tag{26}$$

Substitution of equation (26) into equation (25) gives

$$f(\boldsymbol{r}) = -\frac{1}{k_b^2}\int_\tau \nabla^2 g(\boldsymbol{r}, \boldsymbol{r}_0)d\boldsymbol{r}_0 - \frac{1}{k_b^2}\int_\tau \delta(\boldsymbol{r} - \boldsymbol{r}_0)d\boldsymbol{r}_0. \tag{27}$$

Using the relationship

$$\nabla = -\nabla_0, \tag{28}$$

where subscript 0 stands for the derivative with respect to the source coordinates, one has

$$f(\boldsymbol{r}) = -\frac{1}{k_b^2}\nabla \cdot \int_\tau \nabla_0 g(\boldsymbol{r}, \boldsymbol{r}_0)d\boldsymbol{r}_0 - \frac{1}{k_b^2}D(\boldsymbol{r}), \tag{29}$$

where

$$D(\boldsymbol{r}) = \begin{cases} 1 & \boldsymbol{r} \in \tau \\ 0 & \boldsymbol{r} \notin \tau \end{cases}. \tag{30}$$

Using the theorem, $\int_V \nabla\psi dv = \oint_S \psi d\boldsymbol{s}$, where ψ is an arbitrary scalar function, one can immediately arrive at

$$f(\boldsymbol{r}) = \frac{1}{k_b^2}\nabla \cdot \oint_{\partial\tau} g(\boldsymbol{r}, \boldsymbol{r}_0)\hat{n}(\boldsymbol{r}_0)ds_0 - \frac{1}{k_b^2}D(\boldsymbol{r}), \tag{31}$$

where $\partial\tau$ is the closed surface of the integration volume τ, and $\hat{\boldsymbol{n}}$ is the outgoing unit normal vector of the surface boundary $\partial\tau$.

Following a similar procedure, from equation (25) one obtains

$$\nabla\nabla f(\boldsymbol{r}) = -\nabla \oint_{\partial\tau} g(\boldsymbol{r},\boldsymbol{r}_0)\hat{\boldsymbol{n}}(r_0)ds_0. \tag{32}$$

Substitution of equation (31) and equation (32) into equation (24) yields

$$\overline{\overline{G}}(\boldsymbol{r}) = \frac{1}{\sigma_b}\left[\begin{array}{l} -D(\boldsymbol{r})\overline{\overline{I}} + \overline{\overline{I}}\nabla\cdot\oint_{\partial\tau} g(\boldsymbol{r},\boldsymbol{r}_0)\hat{\boldsymbol{n}}(\boldsymbol{r}_0)ds_0- \\ \nabla\oint_{\partial\tau} g(\boldsymbol{r},\boldsymbol{r}_0)\hat{\boldsymbol{n}}(\boldsymbol{r}_0)ds_0 \end{array}\right]. \tag{33}$$

For the two-dimensional case, the corresponding equation can be derived as

$$\overline{\overline{G}}(\boldsymbol{\rho}) = \frac{1}{\sigma_b}\left[\begin{array}{l} -D(\boldsymbol{\rho})\overline{\overline{I}} + \overline{\overline{I}}\nabla\cdot\oint_{\partial S} g(\boldsymbol{\rho},\boldsymbol{\rho}_0)\hat{\boldsymbol{n}}(\boldsymbol{\rho}_0)dl_0- \\ \nabla\oint_{\partial S} g(\boldsymbol{\rho},\boldsymbol{\rho}_0)\hat{\boldsymbol{n}}(\boldsymbol{\rho}_0)dl_0 \end{array}\right]. \tag{34}$$

where $D(\boldsymbol{\rho})$ is given by

$$D(\boldsymbol{\rho}) = \left\{\begin{array}{ll} 1 & \boldsymbol{\rho} \in S \\ 0 & \boldsymbol{\rho} \notin S \end{array}\right.. \tag{35}$$

So far, we have transformed the volume/surface integral to surface/line integrals. For finite size cells, the distance between the volume surface/surface boundary and the cell center will never be zero, which indicates that by making use of equations (33) and (34), the singularity has been completely eliminated. Another notable advantage of equations (33) and (34) is that they can be used to evaluate the integrals at any point in space, not only the self-interaction term. These formulas provide a way to reduce computing times compared to any alternative numerical method given that the surface/line integral evaluation is much more efficient than the volume/surface integral evaluation.

Equations (33) and (34) are universal for any shape of cell. Depending on the cell shape, $\partial\tau/\partial S$ corresponds to different surfaces/lines, thus different explicit expressions can be obtained. For the 3D case, Appendices D and E give the derivations of the explicit expressions for the integration over a spherical cell and for a general rectangular block cell, respectively.

As shown in Appendix D, the general formula given here leads to exactly the same solution [Equation (16)] as the principal volume

method for a spherical cell. This confirms the validity of the general formula.

For the 2D case, Appendix F gives the derivation of the explicit expressions for the integration over a general rectangular cell (rectangular cylinder).

5. NUMERICAL VALIDATION

For a spherical/circular cell, in Appendices B, C, and D, we show that the new method and the principal volume method give identical analytical expressions. The validity of the new method is apparent for spherical/circular cells.

For a cubic cell, because the accuracy of the equivalent volume approximation is very high [6, 8], we choose to compare the results from the general formula against those obtained from the equivalent volume approximation for a wide range of frequency and discretization cell sizes. The explicit expressions derived in Appendix E are evaluated using a Gauss-Legendre quadrature integration formula. For all the numerical examples considered in this paper, the background Ohmic conductivity σ_b is taken to be $0.5\,\mathrm{S/m}$, and the dielectric constant ε_{rb} is taken to be 1. The frequency range considered is up to $1\,\mathrm{GHz}$. Figure 1 shows simulation results versus $|k_b a|$ for a singular cell, where a is the radius of the equivalent sphere. On that figure, "General Formula" refers to the expressions given in Appendix E, while "PV Appr." refers to equation (16). Because for a cubic cell all the diagonal entries are equal, only the first diagonal entry, G(1,1), is shown on that figure. The upper figure describes the amplitude, while the lower one describes the phase in radians. From Figure 1, one can easily draw the conclusion that the results are perfectly matched, even at very high frequencies. This not only validates the general formula, but also shows that a sphere is truly a very good approximation for a cube with the same volume.

For the measurement points outside the source region, we compare the results between the geometrical factor solution from the equivalent volume approximation [Eq. (19)] and the exact formula presented in this paper. We assume a cell with dimensions $dx = 0.2\,\mathrm{m}$, $dy = 0.2\,\mathrm{m}$, and $dz = 0.2\,\mathrm{m}$, and that the cell is located at the origin. The observation point is located at $(0.2,\ 0.4,\ 0.6)\,\mathrm{m}$, which is intentionally chosen to be very close to the cell. Figures 2 through 4 show the six independent components of the integral tensor. Figure 2 shows G(1,1) and G(1,2); Figure 3 shows G(1,3) and G(2,2); Figure 4 shows G(2,3) and G(3,3). Both amplitude and phase are shown in these figures. The values of the integrals of the Green's function are plotted against $|k_b a|$,
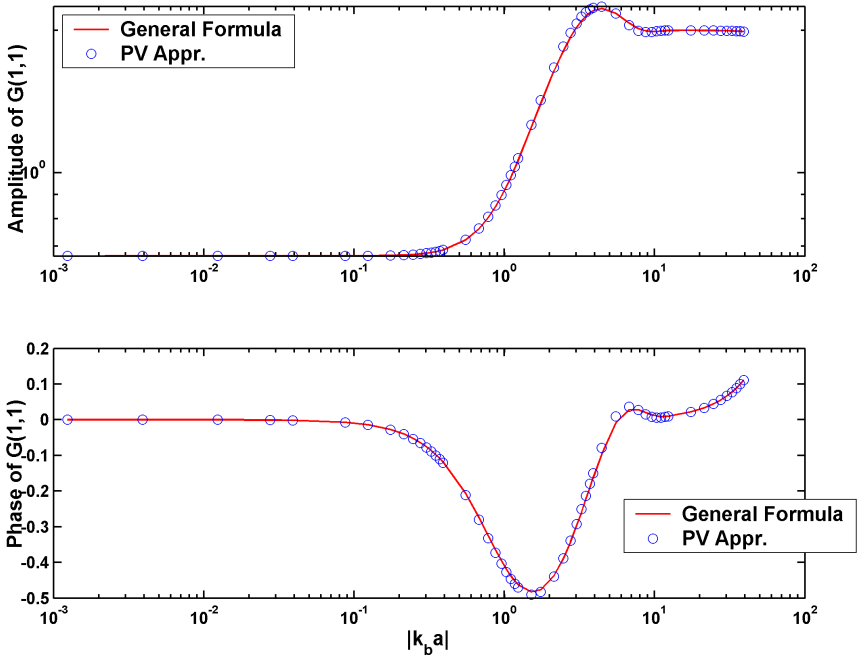
Figure 1. Comparison of integration results obtained from the general formula and the principal-volume approximation assuming a singular cubic cell. The upper panel shows the amplitude, and the bottom panel shows the phase. In both panels, a is the radius of the equivalent sphere.

where a is the distance between the observation point and the center of the cell. Figures 2 through 4 clearly show the accuracy of the geometric factor solution. When $|k_b a|$ is very large, the amplitude of the results reaches the noise level, and a small discrepancy occurs, as shown in Figures 2–4. Because the geometric factor solution is analytical, it is highly efficient from a computational point of view.

For a general rectangular element, the equivalent volume approximation cannot provide accurate results. Intuitively, for a general rectangular cell, the three diagonal entries are not equal, while the equivalent volume approximation can only provide equal diagonal entries. Results from the general formula are compared to those obtained with an already validated code. The code was developed for the computation of the Green's function in a layered medium, and has been optimized to make a compromise between accuracy and
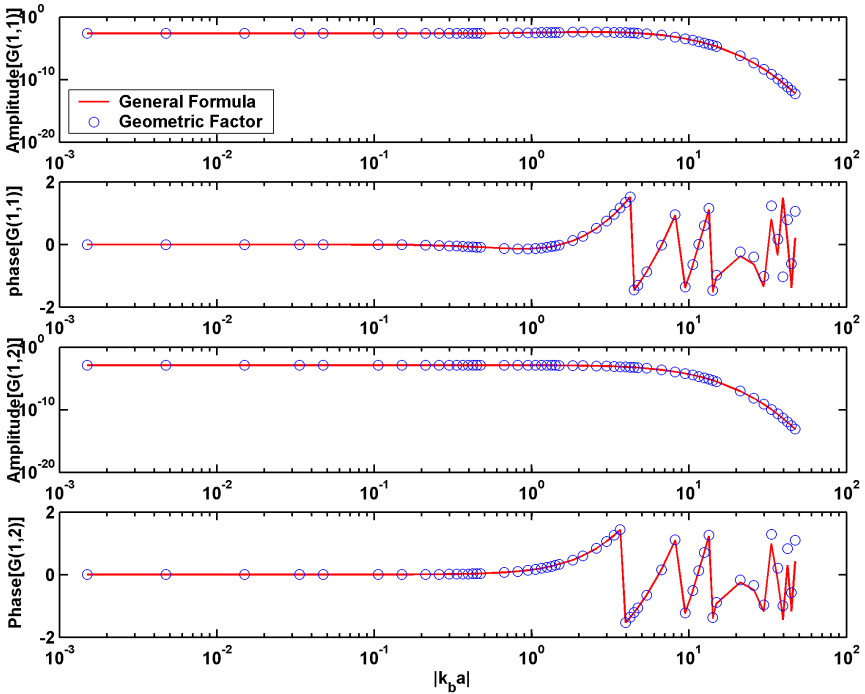
Figure 2. Comparison of integration results obtained from the general formula and from the geometric factor solution assuming a non-singular cubic cell. Two of the six independent components, G(1,1) and G(1,2) are shown on the figure. Both amplitude and phase are shown on the Figure. The cell size is (0.2, 0.2, 0.2) m, and the cell is located at the origin. The observation point is located at (0.2, 0.4, 0.6). In both figures, a is the distance between the cell and the observation point.

computing speed. It is claimed that the code can provide accurate results to the second effective digit. This code is referred to as 'External Code' in this paper. Table 1 gives comparison results for a cell with dimensions $dx = 0.1$ m, $dy = 0.3$ m, and $dz = 0.5$ m. Results for 100 Hz and 1 MHz are listed in the table. The results are clearly matched within 1%. It is believed that the results from the general formula are much more accurate because there is no approximation other than the numerical integration.
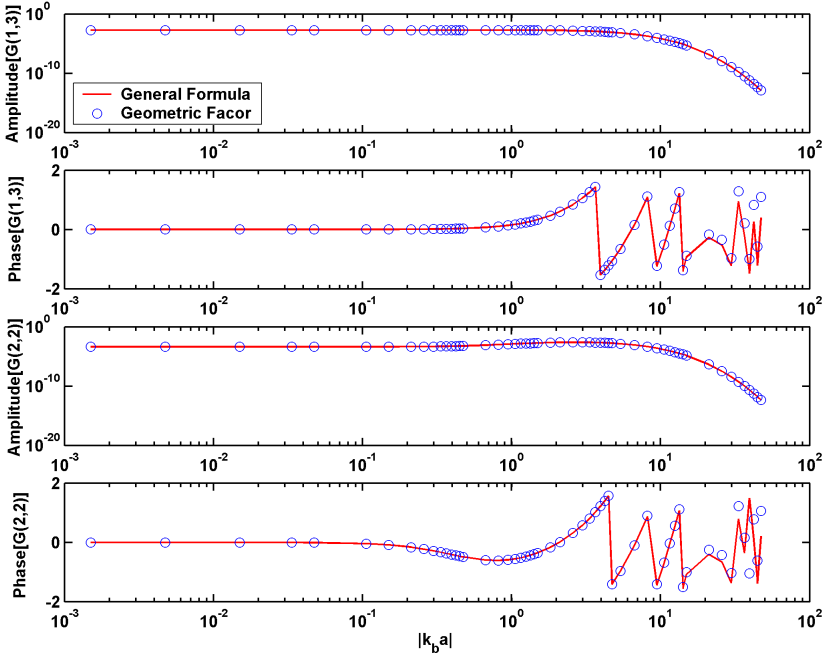
Figure 3. Comparison of integration results obtained from the general formula and from the geometric factor solution assuming a non-singular cubic cell. Two of the six independent components, G(1,3) and G(2,2) are shown on the figure. Both amplitude and phase are shown on the Figure. The cell size is $(0.2, 0.2, 0.2)\,\mathrm{m}$, and the cell is located at the origin. The observation point is located at $(0.2, 0.4, 0.6)$. On both figures, a is the distance between the cell and the observation point.

6. CONCLUSIONS

We have developed a technique for the accurate and efficient evaluation of integrals of the dyadic Green's function without the use of an exclusion volume. The formulas presented in this paper can be used for any cell shape and for any frequency. Explicit expressions have been derived in 3D for a spherical cell and for a general rectangular block and in 2D for a circular cell and a general rectangular cell. We also derived the geometrical factor solution for a spherical cell and a cubic cell. The general integration formula presented in this paper is universal for any cell shape and frequency. The geometrical factor solution can provide accurate results for cubic/square cells, and for a wide range of frequencies.
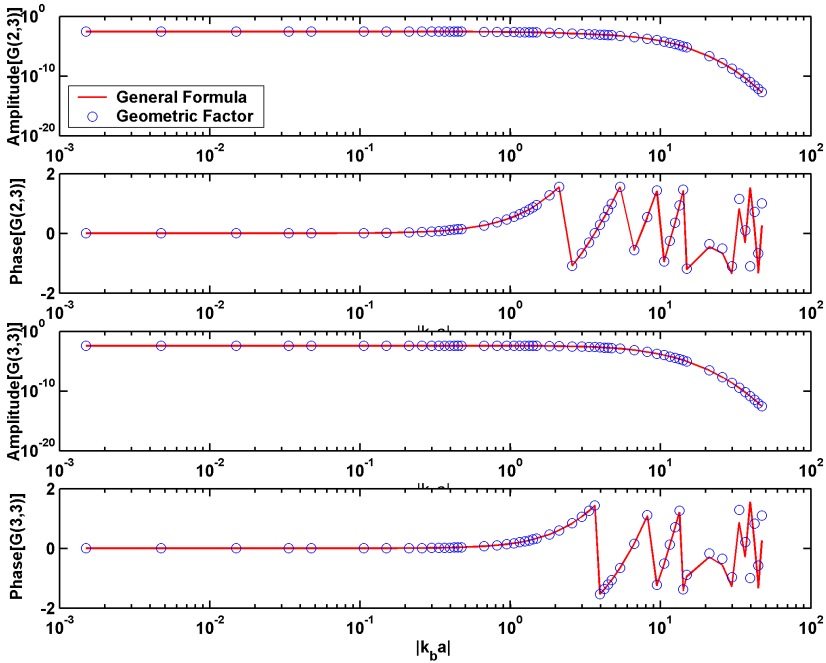
Figure 4. Comparison of integration results obtained from the general formula and from the geometric factor solution assuming a non-singular cubic cell. Two of the six independent components, G(2,3) and G(3,3) are shown on the figure. Both amplitude and phase are shown on the Figure. The cell size is $(0.2, 0.2, 0.2)$ m, and the cell is located at the origin. The observation point is located at $(0.2, 0.4, 0.6)$. In both figures, a is the distance between the cell and the observation point.

ACKNOWLEDGMENT

Table 1. Comparison of integration results obtained with the general formula and with an external code assuming a rectangular block of a dimension (0.1, 0.3, 0.5) m. The external code has been previously validated to render accurate results described to the second effective digit. Results from two frequencies, i.e., 100 Hz and 1 MHz are shown in the table.

		External Code		General Formula	
Freq (Hz)	Quantity	Real Part	Imaginary Part	Real Part	Imaginary Part
100	G(1,1)	-1.52296340	4.1860558E-06	-1.521676900	4.158624051E-06
	G(2,2)	-0.34986061	5.1357538E-06	-0.349633068	5.107571269E-06
	G(3,3)	-0.12866613	5.7510060E-06	-0.128690049	5.722195510E-06
1M	G(1,1)	-1.52979820	3.3293307E-02	-1.528510330	3.301968426E-02
	G(2,2)	-0.35686129	4.2770579E-02	-0.356630176	4.248940200E-02
	G(3,3)	-0.13590108	4.8885193E-02	-0.135921240	4.859771207E-02

APPENDIX A. DERIVATION OF THE EXPRESSION OF THE EQUIVALENT VOLUME APPROXIMATION FOR A SINGULAR CELL USING THE PRINCIPAL VOLUME METHOD

For a spherical exclusion volume [13],

$$\overline{\overline{L}} = \frac{1}{3}\overline{\overline{I}}, \tag{A1}$$

According to the theory of tensor analysis, the operator $\nabla\nabla$ can be expressed as

$$\nabla\nabla = \sum_{p,q=1}^{3} \hat{\boldsymbol{x}}_p \hat{\boldsymbol{x}}_q \frac{\partial^2}{\partial x_p \partial x_q}. \tag{A2}$$

Thus, equation (3) can be written as

$$G_{pq}^e(\boldsymbol{r}, \boldsymbol{r}_0) = i\omega\mu_0 \left(\delta_{pq} + \frac{1}{k_b^2} \frac{\partial^2}{\partial x_p^0 \partial x_q^0} \right) g(\boldsymbol{r}, \boldsymbol{r}_0). \tag{A3}$$

Note that the derivatives indicated in equation (A3) have been transformed into those taken with respect to source coordinates.

By combining equations (A1), (A2) and (A3), equation (12) becomes

$$
\begin{aligned}
G_{pq}(\boldsymbol{r}) &= PV \int_\tau G^e_{pq}(\boldsymbol{r}, \boldsymbol{r}_0) d\boldsymbol{r}_0 - \frac{1}{3\sigma_b}\delta_{pq} \\
&= i\omega\mu_0 PV \int_\tau \delta_{pq} g(\boldsymbol{r}, \boldsymbol{r}_0) d\boldsymbol{r}_0 + \frac{1}{\sigma_b} PV \int_\tau \frac{\partial^2 g(\boldsymbol{r}, \boldsymbol{r}_0)}{\partial x^0_p \partial x^0_q} d\boldsymbol{r}_0 - \frac{1}{3\sigma_b}\delta_{pq} \\
&= i\omega\mu_0 D_1 + \frac{1}{\sigma_b} D_2 - \frac{1}{3\sigma_b}\delta_{pq}.
\end{aligned}
\tag{A4}
$$

Case 1: when $p \neq q$, the first term and the third term on the right-hand side of equation (A4) vanish because of the property of the Kronecker δ function. It can also be shown that D_2 vanishes because the derivative of $g(\boldsymbol{r}, \boldsymbol{r}_0)$ with respect to a particular axis is an odd function about that axis due to symmetry of the coordinates [21]. Thus, all the off-diagonal elements become zero.

Case 2: When $p = q$, because $g(\boldsymbol{r}, \boldsymbol{r}_0)$ is a function of $|\boldsymbol{r} - \boldsymbol{r}_0|$ only, one can define a spherical coordinate system centered at $\boldsymbol{r}$. Thus, without loss of generality, we set $\boldsymbol{r} = \mathbf{0}$. It then follows that

$$
g(\boldsymbol{r}, \boldsymbol{r}_0) = g(r_0) = \frac{e^{ik_b r_0}}{4\pi r_0}.
\tag{A5}
$$

In a spherical coordinate system, D_1 can be written as

$$
\begin{aligned}
D_1 &= PV \int_\tau g(\boldsymbol{r}, \boldsymbol{r}_0) \delta_{pq} d\boldsymbol{r}_0 \\
&= \frac{1}{4\pi} \lim_{\eta \to 0} \int_\eta^a r_0 e^{ik_b r_0} dr_0 \int_0^{2\pi} d\phi_0 \int_0^\pi \sin\theta_0 d\theta_0 \\
&= \lim_{\eta \to 0} \int_\eta^a r_0 e^{ik_b r_0} dr_0.
\end{aligned}
\tag{A6}
$$

Integration by parts yields

$$
D_1 = \frac{1}{k_b^2} \left[(1 - ik_b a) e^{ik_b a} - 1 \right].
\tag{A7}
$$

Because of symmetry, D_2 remains invariant under the rotation of the Cartesian coordinates, and this gives [21]

$$
D_2 = PV \int_\tau \frac{\partial^2 g}{\partial x_0^2} d\boldsymbol{r}_0 = PV \int_\tau \frac{\partial^2 g}{\partial y_0^2} d\boldsymbol{r}_0 = PV \int_\tau \frac{\partial^2 g}{\partial z_0^2} d\boldsymbol{r}_0.
\tag{A8}
$$

Therefore,

$$
D_2 = \frac{1}{3} PV \int_\tau \nabla_0^2 g(\boldsymbol{r}, \boldsymbol{r}_0) d\boldsymbol{r}_0.
\tag{A9}
$$

In spherical coordinates,

$$\nabla_0^2 g(r, r_0) = \frac{1}{r_0^2} \frac{\partial}{\partial r_0} \left(r_0^2 \frac{\partial g(r, r_0)}{\partial r_0} \right). \tag{A10}$$

Substitution of equation (A10) into equation (A9), and after some simple manipulations, one obtains

$$D_2 = -\frac{1}{3} \left[(1 - ik_b a) e^{ik_b a} - 1 \right]. \tag{A11}$$

Substitution of equations (A7) and (A11) into equation (A4) yields

$$G_{pq} = \frac{\delta_{pq}}{3\sigma_b} \left[2(1 - ik_b a) e^{ik_b a} - 3 \right]. \tag{A12}$$

APPENDIX B. DERIVATION OF THE ANALYTICAL SOLUTION FOR THE INTEGRALS OF THE DYADIC GREEN'S FUNCTION FOR A SPHERICAL VOLUME

To derive a solution of equation (24) for a sphere, first $g(\boldsymbol{r}, \boldsymbol{r}_0)$ is expanded in terms of the spherical Bessel and Hankel functions [16], namely,

$$
\begin{aligned}
g(\boldsymbol{r}, \boldsymbol{r}_0) = {} & \frac{ik_b}{4\pi} \sum_{n=0}^{\infty} (2n+1) \sum_{m=0}^{n} \chi_m \frac{(n-m)!}{(n+m)!} P_n^m(\cos\theta) P_n^m(\cos\theta_0) \\
& \cdot \cos[m(\phi - \phi_0)] \begin{cases} j_n(k_b r_0) h_n^{(1)}(k_b r) & r \geq r_0 \\ j_n(k_b r) h_n^{(1)}(k_b r_0) & r \leq r_0 \end{cases},
\end{aligned} \tag{B1}
$$

where

$$r = |\boldsymbol{r}|, \tag{B2}$$
$$r_0 = |\boldsymbol{r}_0|, \tag{B3}$$

and

$$\chi_m = \begin{cases} 1 & m = 0 \\ 2 & m \neq 0 \end{cases}. \tag{B4}$$

Assume that the radius of the sphere is equal to a. For convenience, but without loss of generality, we set the origin at the center of the sphere.

B.1. Derivation for a Singular Cell

For a singular cell, r is located within the sphere. Using equation (B1), in spherical coordinates, equation (25) can be written as

$$f(\boldsymbol{r}) = \frac{ik_b}{4\pi} \sum_{n=0}^{\infty} (2n+1) \sum_{m=0}^{n} \chi_m \frac{(n-m)!}{(n+m)!} P_n^m(\cos\theta)$$

$$\cdot \int_0^{2\pi} d\phi_0 \cos[m(\phi-\phi_0)] \int_0^{\pi} d\theta_0 P_n^m(\cos\theta_0) \sin\theta_0$$

$$\cdot \left[j_n(k_b r) \int_r^a r_0^2 h_n^{(1)}(k_b r_0) dr_0 + h_n^{(1)}(k_b r) \int_0^r r_0^2 j_n(k_b r_0) dr_0 \right]. \text{(B5)}$$

From the properties of the sinusoidal functions and Legendre functions, one can easily conclude that in equation (B5) only the zero-th order terms of m and n remain. This leads to

$$f(\boldsymbol{r}) = ik_b \left[j_0(k_b r) \int_r^a dr_0 r_0^2 h_0^{(1)}(k_b r_0) + h_0^{(1)}(k_b r) \int_0^r dr_0 r_0^2 j_0(k_b r_0) \right]. \tag{B6}$$

Making use of the properties

$$j_0(z) = \frac{\sin z}{z}, \tag{B7}$$

and

$$h_0^{(1)}(z) = -\frac{i}{z} e^{iz}, \tag{B8}$$

and after some tedious manipulations, one obtains

$$f(\boldsymbol{r}) = \frac{1}{k_b^2} \left[-1 + (1 - ik_b a) e^{ik_b a} \frac{\sin(k_b r)}{k_b r} \right]. \tag{B9}$$

To derive the expression for a singular cell, we make use of the power series expansion of $\sin(k_b r)$, i.e.,

$$\sin(k_b r) = \sum_{n=1}^{\infty} (-1)^{n+1} \frac{(k_b r)^{2n-1}}{(2n-1)!}. \tag{B10}$$

Substitution of equation (B10) into equation (B9) yields

$$f(\boldsymbol{r}) = \frac{1}{k_b^2} \left[-1 + (1 - ik_b a) e^{ik_b a} \left(1 + \sum_{n=1}^{\infty} (-1)^n \frac{(k_b r)^{2n}}{(2n+1)!} \right) \right]. \tag{B11}$$

From equation (B11), one obtains that

$$\lim_{r \to 0} f(\boldsymbol{r}) = \frac{1}{k_b^2} \left[-1 + (1 - ik_b a) e^{ik_b a} \right]. \tag{B12}$$

and

$$\lim_{r \to 0} \nabla\nabla f(\boldsymbol{r}) = -\frac{1}{3}(1 - ik_b a)e^{ik_b a}\overline{\overline{I}}. \tag{B13}$$

By substituting equations (B12) and (B13) into equation (24), one obtains

$$\overline{\overline{G}}^{self}(\boldsymbol{r}) = \frac{1}{\sigma_b}\left[-1 + \frac{2}{3}(1 - ik_b a)e^{ik_b a}\right]\overline{\overline{I}}. \tag{B14}$$

This last expression is identical to equations (16) and (A12).

B.2. Expression for Non-Singular Cells

When $\boldsymbol{r}$ lies outside of the sphere, r is always greater than r_0. Thus,

$$f(\boldsymbol{r}) = ik_b h_0^{(1)}(k_b r) \int_0^a dr_0 r_0^2 j_0(k_b r_0). \tag{B15}$$

Using equations (B7) and (B8), one easily arrives at

$$f(\boldsymbol{r}) = C^3 \frac{e^{ik_b r}}{4\pi r}, \tag{B16}$$

where

$$C^3 = \frac{4\pi a}{k_b^2}\left[\frac{\sin(k_b a)}{k_b a} - \cos(k_b a)\right]. \tag{B17}$$

Substituting equation (B16) into equation (24) yields

$$\overline{\overline{G}}(\boldsymbol{r}) = C^3\left[i\omega\mu_0\left(\overline{\overline{I}} + \frac{1}{k_b^2}\nabla\nabla\right)\frac{e^{ik_b r}}{4\pi r}\right]. \tag{B18}$$

If the origin is not at the center of the sphere, we assume that the coordinate of the center of the sphere is $\boldsymbol{r}_c$. Equation (B18) then becomes

$$\overline{\overline{G}}(\boldsymbol{r}) = C^3\left[i\omega\mu_0\left(\overline{\overline{I}} + \frac{1}{k_b^2}\nabla\nabla\right)\frac{e^{ik_b|\boldsymbol{r}-\boldsymbol{r}_c|}}{4\pi|\boldsymbol{r}-\boldsymbol{r}_c|}\right]. \tag{B19}$$

By comparing equation (B19) to equation (3), and by using equation (5), one arrives at the expression

$$\overline{\overline{G}}(\boldsymbol{r}) = C^3\overline{\overline{G}}^e(\boldsymbol{r}, \boldsymbol{r}_c), \tag{B20}$$

where

$$\overline{\overline{G}}^e(\boldsymbol{r}, \boldsymbol{r}_c) = i\omega\mu_0\left(\overline{\overline{I}} + \frac{1}{k_b^2}\nabla\nabla\right)\frac{e^{ik_b|\boldsymbol{r}-\boldsymbol{r}_c|}}{4\pi|\boldsymbol{r}-\boldsymbol{r}_c|}, \tag{B21}$$

and C^3 is given by equation (B17).

The interesting feature of equation (B20) is that the integral of the dyadic Green's function is nothing but the dyadic Green's function evaluated at the geometrical center multiplied by a constant. The constant C^3 is a function of the geometry of the cell, which here is referred to as "3D Geometric Factor". For a sphere, a is the radius of the sphere, while for a cubic cell, a is given by

$$a = \left(\frac{3}{4\pi}\right)^{1/3} a_l, \tag{B22}$$

where a_l is the side length of the cube.

APPENDIX C. DERIVATION OF THE ANALYTICAL SOLUTION FOR THE VOLUME INTEGRALS OF THE DYADIC GREEN'S FUNCTION FOR AN INFINITELY LONG CIRCULAR CYLINDER

The integral of the 2D dyadic Green's function over a cross-section S is written as follows

$$\overline{\overline{G}}(\boldsymbol{\rho}) = i\omega\mu_0 \left(\overline{\overline{I}} + \frac{1}{k_b^2}\nabla\nabla\right) f(\boldsymbol{\rho}), \tag{C1}$$

where $f(\boldsymbol{\rho})$ is given by

$$f(\boldsymbol{\rho}) = \frac{i}{4} \int_s H_0^{(1)}(k_b|\boldsymbol{\rho} - \boldsymbol{\rho}_0|)d\boldsymbol{\rho}_0. \tag{C2}$$

Assume that the origin is at the center of the cross-section of the cylinder. Using the addition theorem of Hankel functions [15], one can write

$$H_0^{(1)}(k_b|\boldsymbol{\rho} - \boldsymbol{\rho}_0|) = \begin{cases} \displaystyle\sum_{m=-\infty}^{+\infty} J_m(k_b\rho_0)H_m^{(1)}(k_b\rho)e^{im(\phi-\phi_0)} & \rho \geq \rho_0 \\ \displaystyle\sum_{m=-\infty}^{+\infty} J_m(k_b\rho)H_m^{(1)}(k_b\rho_0)e^{im(\phi-\phi_0)} & \rho \leq \rho_0 \end{cases}, \tag{C3}$$

where

$$\rho = |\boldsymbol{\rho}|, \tag{C4}$$

and

$$\rho_0 = |\boldsymbol{\rho}_0|, \tag{C5}$$

C.1. Evaluation of a Singular Cell

For a singular cell, equation (C2) can be written as

$$f(\boldsymbol{\rho}) = \frac{i\pi}{2} \left[H_0^{(1)}(k_b\rho) \int_0^\rho J_0(k_b\rho_0)\rho_0 d\rho_0 + J_0(k_b\rho) \int_\rho^a H_0^{(1)}(k_b\rho_0)\rho_0 d\rho_0 \right].$$
(C6)

Using the properties of Bessel functions and of their Wronskian, one arrives at

$$f(\boldsymbol{\rho}) = -\frac{1}{k_b^2} + \frac{i\pi a H_1^{(1)}(k_b a)}{2k_b} J_0(k_b\rho).$$
(C7)

To derive the expressions for a singular cell, which means $\boldsymbol{\rho} = \boldsymbol{\rho}_c$ or $\rho \to 0$, we make use of the series expansion of $J_0(k_b\rho)$, i.e.,

$$J_0(k_b\rho) = \sum_{k=0}^\infty (-1)^k \frac{(k_b\rho/2)^{2k}}{k!k!}.$$
(C8)

It then follows that

$$\lim_{\rho\to 0} f(\boldsymbol{\rho}) = -\frac{1}{k_b^2} + \frac{i\pi a H_1^{(1)}(k_b a)}{2k_b},$$
(C9)

and

$$\lim_{\rho\to 0} \nabla\nabla f(\boldsymbol{\rho}) = \frac{-i\pi k_b a}{4} H_1^{(1)}(k_b a)\overline{\overline{I}}_t,$$
(C10)

where

$$\overline{\overline{I}}_t = \hat{\boldsymbol{x}}\hat{\boldsymbol{x}} + \hat{\boldsymbol{y}}\hat{\boldsymbol{y}}.$$
(C11)

Finally, for a singular cell,

$$\overline{\overline{G}}(\boldsymbol{\rho}) = \frac{1}{\sigma_b} \left[-1 + \frac{i\pi k_b a H_1^{(1)}(k_b a)}{4} \right] \overline{\overline{I}} + \frac{1}{\sigma_b} \frac{i\pi k_b a H_1^{(1)}(k_b a)}{4} \hat{\boldsymbol{z}}\hat{\boldsymbol{z}}.$$
(C12)

C.2. Evaluation of Non-Singular Cells

For non-singular cells, ρ is always greater than ρ_0. Thus, in a cylindrical coordinate system, one has

$$f(\boldsymbol{\rho}) = \frac{i\pi}{2} H_0^{(1)}(k_b\rho) \int_0^a J_0(k_b\rho_0)\rho_0 d\rho_0.$$
(C13)

Using the integration formula for Bessel functions, one obtains

$$f(\boldsymbol{\rho}) = \frac{i\pi a}{2k_b} J_1(k_b a) H_0^{(1)}(k_b \rho). \tag{C14}$$

If the origin is not at the center of the cross-section of the cylinder, we assume that $\boldsymbol{\rho}_c$ is the location of the center. Equation (C14) thus becomes

$$f(\boldsymbol{\rho}) = \frac{i\pi a}{2k_b} J_1(k_b a) H_0^{(1)}(k_b |\boldsymbol{\rho} - \boldsymbol{\rho}_c|). \tag{C15}$$

Using equation (10), it follows that

$$f(\boldsymbol{\rho}) = C^2 g(\boldsymbol{\rho}, \boldsymbol{\rho}_c), \tag{C16}$$

where

$$C^2 = \frac{2\pi a}{k_b} J_1(k_b a) \tag{C17}$$

is the geometrical factor of the 2D Green's function.

By substituting equation (C16) into equation (9), one obtains

$$\overline{\overline{G}}(\boldsymbol{\rho}) = C^2 \overline{\overline{G}}^e(\boldsymbol{\rho}, \boldsymbol{\rho}_c). \tag{C18}$$

This result is analogous to that obtained for the integral of the 3D Green's function.

In equation (C17), for a circular cylinder, a is the radius of the cross-section of the cylinder. For a rectangular cylinder, a is given by

$$a = \frac{a_l}{\sqrt{\pi}}, \tag{C19}$$

where a_l is the side length of the cross-section of the cylinder.

APPENDIX D. DERIVATION OF THE EXPLICIT EXPRESSIONS FOR THE INTEGRAL OF THE DYADIC GREEN'S FUNCTION OVER A SPHERICAL CELL FROM THE GENERAL FORMULA

Assume that the sphere has a radius equal to a. According to equation (E26), only $\nu_{xx}^s, \nu_{yy}^s, \nu_{zz}^s$ need to be evaluated. All the off-diagonal elements are zero for a spherical cell. Because of symmetry, the following relation exists for $\nu_{xx}^s, \nu_{yy}^s, \nu_{zz}^s$:

$$\nu_{xx}^s = \nu_{yy}^s = \nu_{zz}^s. \tag{D1}$$

According to equation (33),

$$\nu_{xx}^s + \nu_{yy}^s + \nu_{zz}^s = \nabla \cdot \oint_{\partial\tau} g(\boldsymbol{r},\boldsymbol{r}_0)\hat{\boldsymbol{n}}(\boldsymbol{r}_0)ds_0. \tag{D2}$$

Thus, by combining equations (D1) and (D2), one obtains

$$\nu_{xx}^s = \nu_{yy}^s = \nu_{zz}^s = \frac{1}{3}\nabla \cdot \oint_{\partial\tau} g(\boldsymbol{r},\boldsymbol{r}_0)\hat{\boldsymbol{n}}(\boldsymbol{r}_0)ds_0. \tag{D3}$$

Equation (D3) can also be written as

$$\nu_{xx}^s = \nu_{yy}^s = \nu_{zz}^s = -\frac{1}{3}\oint_{\partial\tau} \nabla_0 \cdot g(\boldsymbol{r},\boldsymbol{r}_0)\hat{\boldsymbol{n}}(\boldsymbol{r}_0)ds_0. \tag{D4}$$

In Cartesian coordinates,

$$\nabla_0 = \frac{\partial}{\partial x_0}\hat{\boldsymbol{x}} + \frac{\partial}{\partial y_0}\hat{\boldsymbol{y}} + \frac{\partial}{\partial z_0}\hat{\boldsymbol{z}}. \tag{D5}$$

One of the relations between the orthonormal vectors in Cartesian coordinates and spherical coordinates is

$$\hat{\boldsymbol{r}}_0 = \hat{\boldsymbol{x}}\sin\theta_0\cos\phi_0 + \hat{\boldsymbol{y}}\sin\theta_0\sin\phi_0 + \hat{\boldsymbol{z}}\cos\theta_0, \tag{D6}$$

and

$$\frac{\partial}{\partial r_0} = \sin\theta_0\cos\phi_0\frac{\partial}{\partial x} + \sin\theta_0\sin\phi_0\frac{\partial}{\partial y} + \cos\theta_0\frac{\partial}{\partial z}. \tag{D7}$$

By making use of equations (D6) and (D7), one can easily arrive at

$$\oint_{\partial\tau} \nabla_0 \cdot g(\boldsymbol{r},\boldsymbol{r}_0)\hat{\boldsymbol{n}}(\boldsymbol{r}_0)ds_0 = \oint_{\partial\tau} \frac{\partial}{\partial r_0}(g(\boldsymbol{r},\boldsymbol{r}_0))ds_0. \tag{D8}$$

Using equation (A5), one obtains

$$\frac{\partial}{\partial r_0}[g(\boldsymbol{r},\boldsymbol{r}_0)] = \frac{\partial}{\partial r_0}[g(r_0)] = \frac{(ik_b r_0 - 1)e^{ik_b r_0}}{4\pi r_0^2}. \tag{D9}$$

Substitution of equation (D9) into equation (D8) yields

$$\oint_{\partial\tau} \nabla_0 \cdot g(\boldsymbol{r},\boldsymbol{r}_0)\hat{\boldsymbol{n}}(\boldsymbol{r}_0)ds_0 = \frac{(ik_b a - 1)e^{ik_b a}}{4\pi a^2}\oint_{\partial\tau} ds_0 = (ik_b a - 1)e^{ik_b a}. \tag{D10}$$

Substitution of equation (D10) into equation (D4) yields

$$\nu_{xx}^s = \nu_{yy}^s = \nu_{zz}^s = \frac{1}{3}(1 - ik_b a)e^{ik_b a}. \tag{D11}$$

By substituting equation (D11) into equation (E26), one arrives at

$$\overline{\overline{G}}^s(\boldsymbol{r}) = \frac{1}{\sigma_b}\left[-1 + \frac{2}{3}(1 - ik_b a)e^{ik_b a}\right]\overline{\overline{I}}. \tag{D12}$$

This last expression is identical to equations (16) and (A12).

APPENDIX E. DERIVATION OF THE EXPLICIT EXPRESSIONS OF THE INTEGRAL OF THE DYADIC GREEN'S FUNCTION OVER A GENERAL RECTANGULAR BLOCK USING THE GENERAL FORMULA

Assume a Cartesian coordinate system in which the center of a rectangular cell is located at (x_c, y_c, z_c), the observation point is located at (x, y, z), and the side lengths of the cell in the x, y, and z directions are $2a$, $2b$, and $2c$, respectively. Equation (33) can be written as

$$\overline{\overline{G}}(\boldsymbol{r}) = \frac{1}{\sigma_b} \Big[-D(\boldsymbol{r})\overline{\overline{I}} + \overline{\overline{I}}\nabla \cdot (l_x(\boldsymbol{r})\hat{\boldsymbol{x}} + l_y(\boldsymbol{r})\hat{\boldsymbol{y}} + l_z(\boldsymbol{r})\hat{\boldsymbol{z}})$$
$$-\nabla(l_x(\boldsymbol{r})\hat{\boldsymbol{x}} + l_y(\boldsymbol{r})\hat{\boldsymbol{y}} + l_z(\boldsymbol{r})\hat{\boldsymbol{z}})\Big], \tag{E1}$$

where

$$l_x(\boldsymbol{r}) = \frac{1}{4\pi} \left[\int_{y_c-b}^{y_c+b} \int_{z_c-c}^{z_c+c} \left(\frac{e^{ik_b R_{x1}}}{R_{x1}} - \frac{e^{ik_b R_{x2}}}{R_{x2}} \right) dz_0 dy_0 \right], \tag{E2}$$

$$l_y(\boldsymbol{r}) = \frac{1}{4\pi} \left[\int_{x_c-a}^{x_c+a} \int_{z_c-c}^{z_c+c} \left(\frac{e^{ik_b R_{y1}}}{R_{y1}} - \frac{e^{ik_b R_{y2}}}{R_{y2}} \right) dz_0 dx_0 \right], \tag{E3}$$

$$l_z(\boldsymbol{r}) = \frac{1}{4\pi} \left[\int_{x_c-a}^{x_c+a} \int_{y_c-b}^{y_c+b} \left(\frac{e^{ik_b R_{z1}}}{R_{z1}} - \frac{e^{ik_b R_{z2}}}{R_{z2}} \right) dy_0 dx_0 \right], \tag{E4}$$

$$R_{x1} = \left[(x - x_c - a)^2 + (y - y_0)^2 + (z - z_0)^2 \right]^{1/2}, \tag{E5}$$

$$R_{x2} = \left[(x - x_c + a)^2 + (y - y_0)^2 + (z - z_0)^2 \right]^{1/2}, \tag{E6}$$

$$R_{y1} = \left[(y - y_c - b)^2 + (x - x_0)^2 + (z - z_0)^2 \right]^{1/2}, \tag{E7}$$

$$R_{y2} = \left[(y - y_c + b)^2 + (x - x_0)^2 + (z - z_0)^2 \right]^{1/2}, \tag{E8}$$

$$R_{z1} = \left[(z - z_c - c)^2 + (y - y_0)^2 + (x - x_0)^2 \right]^{1/2}, \tag{E9}$$

and

$$R_{z2} = \left[(z - z_c + c)^2 + (y - y_0)^2 + (x - x_0)^2 \right]^{1/2}, \tag{E10}$$

By making use of the general expressions for the gradient and divergence, equation (E1) can be recast as

$$\overline{\overline{G}}(\boldsymbol{r}) = \frac{1}{\sigma_b} \left\{ \begin{array}{l} [-D(\boldsymbol{r}) + \nu_{xx}(\boldsymbol{r}) + \nu_{yy}(\boldsymbol{r}) + \nu_{zz}(\boldsymbol{r})]\overline{\overline{I}} - \\ \nu_{xx}(\boldsymbol{r})\hat{\boldsymbol{x}}\hat{\boldsymbol{x}} - \nu_{xy}(\boldsymbol{r})\hat{\boldsymbol{x}}\hat{\boldsymbol{y}} - \nu_{xz}(\boldsymbol{r})\hat{\boldsymbol{x}}\hat{\boldsymbol{z}} - \nu_{yx}\hat{\boldsymbol{y}}\hat{\boldsymbol{x}} - \\ \nu_{yy}\hat{\boldsymbol{y}}\hat{\boldsymbol{y}} - \nu_{yz}\hat{\boldsymbol{y}}\hat{\boldsymbol{z}} - \nu_{zx}\hat{\boldsymbol{z}}\hat{\boldsymbol{x}} - \nu_{zy}\hat{\boldsymbol{z}}\hat{\boldsymbol{y}} - \nu_{zz}\hat{\boldsymbol{z}}\hat{\boldsymbol{z}} \end{array} \right\}, \quad (E11)$$

where the unit dyad $\overline{\overline{I}}$ can be written in terms of three orthonormal vectors

$$\overline{\overline{I}} = \hat{\boldsymbol{x}}\hat{\boldsymbol{x}} + \hat{\boldsymbol{y}}\hat{\boldsymbol{y}} + \hat{\boldsymbol{z}}\hat{\boldsymbol{z}}. \tag{E12}$$

Accordingly, (F11) can be written as

$$\overline{\overline{G}}(\boldsymbol{r}) = \frac{1}{\sigma_b} \left\{ \begin{array}{l} [-D(\boldsymbol{r}) + \nu_{yy}(\boldsymbol{r}) + \nu_{zz}(\boldsymbol{r})]\hat{\boldsymbol{x}}\hat{\boldsymbol{x}} - \nu_{xy}(\boldsymbol{r})\hat{\boldsymbol{x}}\hat{\boldsymbol{y}} - \nu_{xz}(\boldsymbol{r})\hat{\boldsymbol{x}}\hat{\boldsymbol{z}} - \\ \nu_{yx}\hat{\boldsymbol{y}}\hat{\boldsymbol{x}} + [-D(\boldsymbol{r}) + \nu_{xx}(\boldsymbol{r}) + \nu_{zz}(\boldsymbol{r})]\hat{\boldsymbol{y}}\hat{\boldsymbol{y}} - \nu_{yz}\hat{\boldsymbol{y}}\hat{\boldsymbol{z}} - \\ \nu_{zx}\hat{\boldsymbol{z}}\hat{\boldsymbol{x}} - \nu_{zy}\hat{\boldsymbol{z}}\hat{\boldsymbol{y}} + [-D(\boldsymbol{r}) + \nu_{xx}(\boldsymbol{r}) + \nu_{yy}(\boldsymbol{r})]\hat{\boldsymbol{z}}\hat{\boldsymbol{z}} \end{array} \right\}. \tag{E13}$$

Using matrix notation,

$$\overline{\overline{G}}(\boldsymbol{r}) = \frac{1}{\sigma_b}$$

$$\begin{bmatrix} -D(\boldsymbol{r}) + \nu_{yy}(\boldsymbol{r}) + \nu_{zz}(\boldsymbol{r}) & -\nu_{xy}(\boldsymbol{r}) & -\nu_{xz}(\boldsymbol{r}) \\ -\nu_{yx}(\boldsymbol{r}) & -D(\boldsymbol{r}) + \nu_{xx}(\boldsymbol{r}) + \nu_{zz}(\boldsymbol{r}) & -\nu_{yz}(\boldsymbol{r}) \\ -\nu_{zx}(\boldsymbol{r}) & -\nu_{zy}(\boldsymbol{r}) & -D(\boldsymbol{r}) + \nu_{xx}(\boldsymbol{r}) + \nu_{yy}(\boldsymbol{r}) \end{bmatrix}, \tag{E14}$$

where

$$\begin{aligned} \nu_{xx}(\boldsymbol{r}) &= \frac{\partial}{\partial x}[l_x(\boldsymbol{r})] \\ &= \frac{1}{4\pi} \left[\int_{y_c-b}^{y_c+b} \int_{z_c-c}^{z_c+c} \left(\frac{(x - x_c - a)e^{ik_b R_{x1}}(ik_b R_{x1} - 1)}{R_{x1}^3} \right. \right. \\ &\quad \left. \left. - \frac{(x - x_x + a)e^{ik_b R_{x2}}(ik_b R_{x2} - 1)}{R_{x2}^3} \right) dz_0 dy_0 \right], \quad (E15) \end{aligned}$$

$$\begin{aligned} \nu_{yy}(\boldsymbol{r}) &= \frac{\partial}{\partial y}[l_y(\boldsymbol{r})] \\ &= \frac{1}{4\pi} \left[\int_{x_c-a}^{x_c+a} \int_{z_c-c}^{z_c+c} \left(\frac{(y - y_c - b)e^{ik_b R_{y1}}(ik_b R_{y1} - 1)}{R_{y1}^3} \right. \right. \\ &\quad \left. \left. - \frac{(y - y_c + a)e^{ik_b R_{y2}}(ik_b R_{y2} - 1)}{R_{y2}^3} \right) dz_0 dx_0 \right], \quad (E16) \end{aligned}$$

$$\nu_{zz}(\boldsymbol{r}) = \frac{\partial}{\partial z}[l_z(\boldsymbol{r})]$$

$$= \frac{1}{4\pi}\left[\int_{x_c-a}^{x_c+a}\int_{y_c-b}^{y_c+b}\left(\frac{(z-z_c-c)e^{ik_bR_{z1}}(ik_bR_{z1}-1)}{R_{z1}^3}\right.\right.$$

$$\left.\left.- \frac{(z-z_c+c)e^{ik_bR_{z2}}(ik_bR_{z2}-1)}{R_{z2}^3}\right)dy_0dx_0\right], \quad \text{(E17)}$$

$$\nu_{yx}(\boldsymbol{r}) = \frac{\partial}{\partial y}[l_x(\boldsymbol{r})]$$

$$= \frac{1}{4\pi}\left[\int_{y_c-b}^{y_c+b}\int_{z_c-c}^{z_c+c}(y-y_0)\left(\frac{e^{ik_bR_{x1}}(ik_bR_{x1}-1)}{R_{x1}^3}\right.\right.$$

$$\left.\left.- \frac{e^{ik_bR_{x2}}(ik_bR_{x2}-1)}{R_{x2}^3}\right)dz_0dy_0\right], \quad \text{(E18)}$$

$$\nu_{zx}(\boldsymbol{r}) = \frac{\partial}{\partial z}[l_x(\boldsymbol{r})]$$

$$= \frac{1}{4\pi}\left[\int_{y_c-b}^{y_c+b}\int_{z_c-c}^{z_c+c}(z-z_0)\left(\frac{e^{ik_bR_{x1}}(ik_bR_{x1}-1)}{R_{x1}^3}\right.\right.$$

$$\left.\left.- \frac{e^{ik_bR_{x2}}(ik_bR_{x2}-1)}{R_{x2}^3}\right)dz_0dy_0\right], \quad \text{(E19)}$$

$$\nu_{xy}(\boldsymbol{r}) = \frac{\partial}{\partial x}[l_y(\boldsymbol{r})]$$

$$= \frac{1}{4\pi}\left[\int_{x_c-a}^{x_c+a}\int_{z_c-c}^{z_c+c}(x-x_0)\left(\frac{e^{ik_bR_{y1}}(ik_bR_{y1}-1)}{R_{y1}^3}\right.\right.$$

$$\left.\left.- \frac{e^{ik_bR_{y2}}(ik_bR_{y2}-1)}{R_{y2}^3}\right)dz_0dx_0\right], \quad \text{(E20)}$$

$$\nu_{zy}(\boldsymbol{r}) = \frac{\partial}{\partial z}[l_y(\boldsymbol{r})]$$

$$= \frac{1}{4\pi}\left[\int_{x_c-a}^{x_c+a}\int_{z_c-c}^{z_c+c}(z-z_0)\left(\frac{e^{ik_bR_{y1}}(ik_bR_{y1}-1)}{R_{y1}^3}\right.\right.$$

$$\left.\left.- \frac{e^{ik_bR_{y2}}(ik_bR_{y2}-1)}{R_{y2}^3}\right)dz_0dx_0\right], \quad \text{(E21)}$$

$$\nu_{xz}(\boldsymbol{r}) = \frac{\partial}{\partial x}[l_z(\boldsymbol{r})]$$

$$= \frac{1}{4\pi}\left[\int_{x_c-a}^{x_c+a}\int_{y_c-b}^{y_c+b}(x-x_0)\left(\frac{e^{ik_bR_{z1}}(ik_bR_{z1}-1)}{R_{z1}^3}\right.\right.$$

$$\left.\left. - \frac{e^{ik_bR_{z2}}(ik_bR_{z2}-1)}{R_{z2}^3}\right)dy_0dx_0\right], \tag{E22}$$

$$\nu_{yz}(\boldsymbol{r}) = \frac{\partial}{\partial y}[l_z(\boldsymbol{r})]$$

$$= \frac{1}{4\pi}\left[\int_{x_c-a}^{x_c+a}\int_{y_c-b}^{y_c+b}(y-y_0)\left(\frac{e^{ik_bR_{z1}}(ik_bR_{z1}-1)}{R_{z1}^3}\right.\right.$$

$$\left.\left. - \frac{e^{ik_bR_{z2}}(ik_bR_{z2}-1)}{R_{z2}^3}\right)dy_0dx_0\right], \tag{E23}$$

and $D(\boldsymbol{r})$ is given by equation (30). It can be easily shown that

$$\begin{aligned}\nu_{xy} &= \nu_{yx}\\ \nu_{xz} &= \nu_{zx}.\\ \nu_{yz} &= \nu_{zy}\end{aligned} \tag{E24}$$

Equation (E15) is valid for any observation-point locations.

When $\boldsymbol{r} = \boldsymbol{r}_0$, $R_{x1} = R_{x2}$, $R_{y1} = R_{y2}$, and $R_{z1} = R_{z2}$, one obtains

$$\nu_{xy} = \nu_{xz} = \nu_{yz} = 0, \tag{E25}$$

which is identical to the conclusion drawn from Appendix A when $p \neq q$.

Therefore, for a singular cell one obtains

$$\overline{\overline{G}}^s(\boldsymbol{s}) = \frac{1}{\sigma_b}$$

$$\begin{bmatrix} -1+\nu_{yy}^s(\boldsymbol{r})+\nu_{zz}^s(\boldsymbol{r}) & 0 & 0 \\ 0 & -1+\nu_{xx}^s(\boldsymbol{r})+\nu_{zz}^s(\boldsymbol{r}) & 0 \\ 0 & 0 & -1+\nu_{xx}^s(\boldsymbol{r})+\nu_{yy}^s(\boldsymbol{r}) \end{bmatrix}, \tag{E26}$$

where

$$\nu_{xx}^s(\boldsymbol{r}) = -\frac{a}{2\pi}\left[\int_{-b}^{b}\int_{-c}^{c}\left(\frac{e^{ik_bR_x}(ik_bR_x-1)}{R_x^2}\right)dz_0dy_0\right], \tag{E27}$$

$$\nu_{yy}^s(\boldsymbol{r}) = -\frac{b}{2\pi}\left[\int_{-a}^{a}\int_{-c}^{c}\left(\frac{e^{ik_bR_y}(ik_bR_y-1)}{R_y^2}\right)dz_0dx_0\right], \quad \text{(E28)}$$

$$\nu_{zz}^s(\boldsymbol{r}) = -\frac{c}{2\pi}\left[\int_{-a}^{a}\int_{-b}^{b}\left(\frac{e^{ik_bR_z}(ik_bR_z-1)}{R_z^2}\right)dy_0dx_0\right], \quad \text{(E29)}$$

$$R_x = \left[a^2+y_0^2+z_0^2\right]^{1/2}, \tag{E30}$$

$$R_y = \left[b^2+x_0^2+z_0^2\right]^{1/2}, \tag{E31}$$

and

$$R_z = \left[c^2+x_0^2+y_0^2\right]^{1/2}. \tag{E32}$$

APPENDIX F. DERIVATION OF THE EXPLICIT EXPRESSIONS FOR THE INTEGRAL OF THE DYADIC GREEN'S FUNCTION OVER A GENERAL RECTANGULAR CELL (RECTANGULAR CYLINDER)

Using vector and tensor analysis techniques, equation (34) can be written as,

$$\overline{\overline{G}}(\boldsymbol{\rho}) = \frac{1}{\sigma_b}\left\{\left\{-D(\boldsymbol{\rho})+\nabla\cdot[l_x(\boldsymbol{\rho})\hat{\boldsymbol{x}}+l_y(\boldsymbol{\rho})\hat{\boldsymbol{y}}]\right\}\overline{\overline{I}}-\nabla[l_x(\boldsymbol{\rho})\hat{\boldsymbol{x}}+l_y(\boldsymbol{\rho})\hat{\boldsymbol{y}}]\right\}. \tag{F1}$$

Assume that the location of the center of the rectangular cell is

$$\boldsymbol{\rho}_c = x_c\hat{\boldsymbol{x}} + y_c\hat{\boldsymbol{y}}, \tag{F2}$$

and that the lengths of the rectangular cells are $2a$ and $2b$ in the x and y directions, respectively. It then follows that

$$l_x(\boldsymbol{\rho}) = \frac{i}{4}\left[\int_{y_c-b}^{y_c+b}\left(H_0^{(1)}(k_b\rho_{x1})-H_0^{(1)}(k_b\rho_{x1})\right)dy_0\right], \tag{F3}$$

and

$$l_y(\boldsymbol{\rho}) = \frac{i}{4}\left[\int_{x_c-a}^{x_c+a}\left(H_0^{(1)}(k_b\rho_{y1})-H_0^{(1)}(k_b\rho_{y1})\right)dx_0\right], \tag{F4}$$

where

$$\rho_{x1} = \sqrt{(x-x_c-a)^2+(y-y_0)^2}, \tag{F5}$$

$$\rho_{x2} = \sqrt{(x-x_c+a)^2+(y-y_0)^2}, \tag{F6}$$

$$\rho_{y1} = \sqrt{(y-y_c-b)^2+(x-x_0)^2}, \tag{F7}$$

and

$$\rho_{y2} = \sqrt{(y - y_c + b)^2 + (x - x_0)^2}. \tag{F8}$$

Substitution of these last expressions into equation (F1) yields

$$\overline{\overline{G}}(\boldsymbol{\rho}) = \frac{1}{\sigma_b} \left\{ \begin{array}{l} [-D(\boldsymbol{\rho}) + \nu_{yy}(\boldsymbol{\rho})]\hat{\boldsymbol{x}}\hat{\boldsymbol{x}} - \nu_{xy}(\boldsymbol{\rho})\hat{\boldsymbol{x}}\hat{\boldsymbol{y}} - \\ \nu_{yx}(\boldsymbol{\rho})\hat{\boldsymbol{y}}\hat{\boldsymbol{x}} + [-D(\boldsymbol{\rho}) + \nu_{xx}(\boldsymbol{\rho})]\hat{\boldsymbol{y}}\hat{\boldsymbol{y}} + \\ [-D(\boldsymbol{\rho}) + \nu_{xx}(\boldsymbol{\rho}) + \nu_{yy}(\boldsymbol{\rho})]\hat{\boldsymbol{z}}\hat{\boldsymbol{z}} \end{array} \right\}, \tag{F9}$$

or, in matrix notation,

$$\overline{\overline{G}}(\boldsymbol{\rho}) = \frac{1}{\sigma_b}$$
$$\begin{pmatrix} -D(\boldsymbol{\rho}) + \nu_{yy}(\boldsymbol{\rho}) & -\nu_{xy}(\boldsymbol{\rho}) & 0 \\ -\nu_{yx}(\boldsymbol{\rho}) & -D(\boldsymbol{\rho}) + \nu_{xx}(\boldsymbol{\rho}) & 0 \\ 0 & 0 & -D(\boldsymbol{\rho}) + \nu_{xx}(\boldsymbol{\rho}) + \nu_{yy}(\boldsymbol{\rho}) \end{pmatrix}, \tag{F10}$$

where

$$\begin{aligned} \nu_{xx}(\boldsymbol{\rho}) &= \frac{\partial}{\partial x}(l_x(\boldsymbol{\rho})) \\ &= -\frac{ik_b}{4} \left\{ \int_{y_c-b}^{y_c+b} \left[\frac{(x - x_c - a)H_1^{(1)}(k_b\rho_{x1})}{\rho_{x1}} \right. \right. \\ &\qquad \left. \left. - \frac{(x - x_c + a)H_1^{(1)}(k_b\rho_{x2})}{\rho_{x2}} \right] dy_0 \right\}, \tag{F11} \end{aligned}$$

$$\begin{aligned} \nu_{yy}(\boldsymbol{\rho}) &= \frac{\partial}{\partial y}(l_y(\boldsymbol{\rho})) \\ &= -\frac{ik_b}{4} \left\{ \int_{x_c-a}^{x_c+a} \left[\frac{(y - y_c - b)H_1^{(1)}(k_b\rho_{y1})}{\rho_{y1}} \right. \right. \\ &\qquad \left. \left. - \frac{(y - y_c + b)H_1^{(1)}(k_b\rho_{y2})}{\rho_{y2}} \right] dx_0 \right\}, \tag{F12} \end{aligned}$$

and

$$\begin{aligned} \nu_{xy}(\boldsymbol{\rho}) = \nu_{yx}(\boldsymbol{\rho}) &= \frac{\partial}{\partial x}(l_y(\boldsymbol{\rho})) \\ &= -\frac{i}{4}\left\{ H_0^{(1)}(k_b\rho_{xy1}) - H_0^{(1)}(k_b\rho_{xy2}) + H_0^{(1)}(k_b\rho_{xy3}) - H_0^{(1)}(k_b\rho_{xy4}) \right\}, \tag{F13} \end{aligned}$$

where

$$\rho_{xy1} = \sqrt{(x - x_c - a)^2 + (y - y_c - b)^2}, \tag{F14}$$

$$\rho_{xy2} = \sqrt{(x - x_c - a)^2 + (y - y_c + b)^2}, \tag{F15}$$

$$\rho_{xy3} = \sqrt{(x - x_c + a)^2 + (y - y_c + b)^2}, \tag{F16}$$

and

$$\rho_{xy4} = \sqrt{(x - x_c + a)^2 + (y - y_c - b)^2}. \tag{F17}$$

In equation (F10),

$$D(\boldsymbol{\rho}) = \begin{cases} 1 & \text{self cell} \\ 0 & \text{otherwise} \end{cases}. \tag{F18}$$

For a self-cell, one has

$$\overline{\overline{G}}^s(\boldsymbol{\rho}) = \frac{1}{\sigma_b} \begin{pmatrix} -1 + \nu_{yy}^s(\boldsymbol{\rho}) & 0 & 0 \\ 0 & -1 + \nu_{xx}^s(\boldsymbol{\rho}) & 0 \\ 0 & 0 & -1 + \nu_{xx}^s(\boldsymbol{\rho}) + \nu_{yy}^s(\boldsymbol{\rho}) \end{pmatrix}, \tag{F19}$$

where

$$\nu_{xx}^s(\boldsymbol{\rho}) = \frac{ik_b a}{2} \left\{ \int_{-b}^{b} \left[\frac{H_1^{(1)}(k_b \rho_x)}{\rho_x} \right] dy_0 \right\}, \tag{F20}$$

$$\nu_{yy}^s(\boldsymbol{\rho}) = \frac{ik_b b}{2} \left\{ \int_{-a}^{a} \left[\frac{H_1^{(1)}(k_b \rho_y)}{\rho_y} \right] dx_0 \right\}, \tag{F21}$$

$$\rho_x = \sqrt{a^2 + y_0^2}, \tag{F22}$$

and

$$\rho_y = \sqrt{b^2 + x_0^2}. \tag{F23}$$

REFERENCES

1. Chew, W. C., "Some observations on the spatial and eigenfunction representations of dyadic Green's functions," *IEEE Trans. Antennas Propagat.*, Vol. 37, 1322–1327, 1989.
2. Van Bladel, J., "Some remarks on Green's dyadic for infinite space," *IEEE Trans. Antennas Propagat.*, Vol. 9, 563–566, 1961.

3. Yaghjian, A. D., "Electric dyadic Green's functions in the source region," *Proc. IEEE*, Vol. 68, 248–263, 1980.

4. Yaghjian, A. D., "A delta-distribution derivation of the electric field in the source region," *Electromagn.*, Vol. 2, 161–167, 1982.

5. Su, C. C., "A simple evaluation of some principal value integrals for dyadic Green's function using symmetry property," *IEEE Trans. Antennas Propagat.*, Vol. AP-35, No. 11, 1306–1307, 1987.

6. Lee, S. W., J. Boersma, C. L. Law, and G. A. Deschamps, "Singularity in Green's function and its numerical evaluation," *IEEE Trans. Antennas Propagat.*, Vol. 28, 311–317, 1980.

7. Harrington, R. F., *Field Computation by Moment Methods*, Macmillan, New York, 1968.

8. Livesay, D. E. and K.-M. Chen, "Electromagnetic fields induced inside arbitrarily shaped biological bodies," *IEEE Trans. Microwave Theory Tech.*, Vol. MTT-22, No. 12, 1273–1280, 1974.

9. Fang, S., G. Gao, and C. Torres-Verdín, "Efficient 3-D electromagnetic modeling in the presence of anisotropic conductive media using integral equations," *Proceedings of the Third International Three-Dimensional Electromagnetics (3DEM-3) Symposium*, J. Macnae and G. Liu, Australian Society of Exploration Geophysicist, 2003.

10. Gao, G., S. Fang, and C. Torres-Verdín, "A new approximation for 3D electromagnetic scattering in the presence of anisotropic conductive media," *Proceedings of the Third International Three-Dimensional Electromagnetics (3DEM-3) Symposium*, J. Macnae and G. Liu, Australian Society of Exploration Geophysicist, 2003.

11. Gao, G., C. Torres-Verdín, and S. Fang, "Fast 3D modeling of borehole induction data in dipping and anisotropic formations using a novel approximation technique," *Petrophysics*, Vol. 45, 335–349, 2004.

12. Hohmann, G. W., "Three-dimensional induced polarization and electromagnetic modelling," *Geophysics*, Vol. 40, No. 2, 309–324, 1975.

13. Chew, W. C., *Waves and Fields in Inhomogeneous Media*, Van Nostrand Reinhold, New York, 1990.

14. Hoekstra, A., J. Rahola, and P. Sloot, "Accuracy of internal fields in volume integral equation simulations of light scattering," *Applied Optics*, Vol. 37, No. 36, 1998.

15. Torres-Verdín, C. and T. M. Habashy, "Rapid 2.5-dimensional forward modeling and inversion via a new nonlinear scattering approximation," *Radio Science*, Vol. 29, No. 4, 1051–1079, 1994.

16. Habashy, T. M., R. W. Groom, and B. Spies, "Beyond the Born and Rytov approximations: A nonlinear approach to electromagnetic scattering," *J. Geophys. Res.*, Vol. 98, No. B2, 1759–1775, 1993.

Guozhong Gao is currently a Ph.D. candidate and Graduate Research Assistant in the Department of Petroleum and Geosystems Engineering of The University of Texas at Austin. He obtained his Bachelor's degree and Master's degree from Southwest Petroleum Institute (China) and the University of Petroleum in Beijing in 1996 and 2000, respectively, all in Applied Geophysics. His current research interests include electromagnetic modeling in inhomogeneous and anisotropic media, numerical simulation, inverse scattering, and integrated formation evaluation and reservoir characterization. Email: zhong@mail.utexas.edu.

Carlos Torres-Verdín received a Ph.D. in Engineering Geoscience from the University of California, Berkeley, in 1991. During 1991–1997, he held the position of Research Scientist with Schlumberger-Doll Research. From 1997–1999, he was Reservoir Specialist and Technology Champion with YPF (Buenos Aires, Argentina). Since 1999, he has been with the Department of Petroleum and Geosystems Engineering of The University of Texas at Austin, where he conducts research in formation evaluation and integrated reservoir characterization. Dr. Torres-Verdín currently holds the position of Associate Professor. He has served as Guest Editor for Radio Science, and is currently a member of the Editorial Board of the Journal of Electromagnetic Waves and Applications, and an associate editor for Petrophysics (SPWLA) and the SPE Journal. Email: cverdin@uts.cc.utexas.edu.

Tarek M. Habashy received the B.Sc. degree from Cairo University, Egypt, and the M.Sc. and Ph.D. degrees from Massachusetts Institute of Technology (MIT), Cambridge, in 1976, 1980, and 1983, respectively, all in electrical engineering. During the academic year 1982–1983, he was a Research Associate in the Department of Electrical Engineering and Computer Science, MIT. Since September 1983, he has been with Schlumberger-Doll Research, Ridgefield, CT, and is now the Director of Mathematic and Modeling Department. He is also a Scientific Advisor there, conducting research in electromagnetic waves and fields, dielectric and resistivity logging tools and techniques, inverse scattering theory, antenna theory and design, mixed boundary value

problems, and numerical analysis. He served as a Editor of Radio Science and as a member of the advisory committee board of the book series Progress in Electromagnetic Research. He is currently a member of the editorial boards of Inverse Problems and the Journal of Electromagnetic Waves and Applications.